Proceedings of Eurotherm78 - Computational Thermal Radiation in Participating Media II
5-7 April 2006, Poitiers, France

Direct Numerical Simulation of Turbulence−Radiation Interactions in a Statistically One-dimensional Nonpremixed System

by K. V. DESHMUKH, M. F. MODEST *, and D. C. HAWORTH

Department of Mechanical and Nuclear Engineering
The Pennsylvania State University
University Park, PA 16802 USA
**email: MFModest@psu.edu*

Abstract
An important issue in chemically reacting turbulent flows is the interaction between turbulence and radiation (TRI), which arises from highly nonlinear coupling between fluctuations in temperature and species composition of the flow field with the fluctuations of radiative intensity. Here direct numerical simulation (DNS) has been employed to investigate TRI in canonical nonpremixed systems in three-dimensional geometries. A photon Monte Carlo method has been used to solve the radiative transfer equation (RTE), which has been coupled with the flow solver. Radiation properties employed here correspond to a nonscattering fictitious gray gas with a Planck-mean absorption coefficient, which mimics that of typical hydrocarbon−air combustion products. Individual contributions of emission and absorption TRI have been isolated and quantified. The temperature self-correlation, the absorption coefficient−Planck function correlation, and the absorption coefficient−intensity correlation have been examined for small-to-large values of the optical thickness, and contributions from all three correlations have been found to be significant at intermediate-to-large values of optical thickness while only the temperature self-correlation and the absorption coefficient−Planck function correlation are significant for the optically thin limit.

1. Introduction

Most practical combustion devices involve turbulent fluid flow, and the high temperatures prevalent in most combustion processes result in substantial heat transfer by radiation. Accurate description of turbulence and combustion by themselves is mathematically complex and computationally expensive. This has often resulted in the neglect of radiation, or the treatment of radiation using simple models in turbulent combustion applications, to avoid the additional complexity of solving the radiative transfer equation (RTE) [1].

The importance of interactions between turbulence and thermal radiation (turbulence−radiation interactions or TRI) has long been recognized [2–8]. TRI is known to result in increased radiative emission, reduced temperatures and, consequently, significant changes in key pollutant species (particularly NOx and soot) in chemically reacting turbulent flows. TRI arises from the highly nonlinear coupling between temperature, composition and radiative intensity fluctuations. Mazumder and Modest [7], and Li and Modest [8] showed an approximately 30%

increase in radiative flux with TRI compared to thermal radiation without TRI in their modeling studies of nonpremixed turbulent jet flames. Coelho [9] reported a nearly 50% increase in radiative heat loss due to TRI for a nonpremixed methane$-$air turbulent jet flame, while Tessé et al. [10] reported a 30% increase in radiative heat loss with consideration of TRI for a sooty, nonpremixed ethylene$-$air turbulent jet flame. Wu et al. [11] were the first to study TRI for an idealized turbulent premixed flame using direct numerical simulation (DNS) coupled with a photon Monte Carlo method for the solution of the RTE; they found that emission and absorption are both enhanced when TRI are considered, and that both effects remained important even at relatively low optical thicknesses.

Here DNS coupled with a radiation photon Monte Carlo method [11, 12] is used to isolate and quantify TRI effects in a statistically one-dimensional nonpremixed system. The aims are to provide new fundamental physical insight into TRI in chemically reacting turbulent flows and to provide guidance for model development. The nature of turbulence$-$radiation interactions is discussed in Section 2; the model problem is outlined in Section 3, and results and a discussion are provided in Section 4.

2. Turbulence$-$Radiation Interactions in Chemically Reacting Flows

The radiation source term in the instantaneous energy equation can be expressed as the divergence of the radiative heat flux $\vec{q}_{rad}$. For the special case of a gray medium,

$$\nabla \cdot \vec{q}_{rad} = 4\kappa_P \sigma T^4 - \kappa_P G \; , \tag{1}$$

where κ_P is the Planck-mean absorption coefficient [1], σ is the Stefan-Boltzmann constant and G the direction-integrated incident radiation. The first term on the right-hand side of Eq. (1) corresponds to emission and the second to absorption. TRI is brought into evidence by taking the mean of Eq. (1):

$$\langle \nabla \cdot \vec{q}_{rad} \rangle = 4\sigma \langle \kappa_P T^4 \rangle - \langle \kappa_P G \rangle \; , \tag{2}$$

where angled brackets denote mean quantities.

In the emission term, TRI appears as a correlation between the Planck-mean absorption coefficient and the fourth power of temperature (the spectrally integrated Planck function, I_b): $\langle \kappa_P T^4 \rangle = \langle \kappa_P \rangle \langle T^4 \rangle + \langle \kappa_P' \cdot (T^4)' \rangle$, where a prime denotes a fluctuation about the local mean. Emission TRI can be decomposed into the temperature self-correlation ($\langle T^4 \rangle \neq \langle T \rangle^4$) and the absorption coefficient$-$Planck function correlation. In the absorption term, TRI appears as a correlation between the absorption coefficient and the intensity (or incident radiation), $\langle \kappa_P G \rangle = \langle \kappa_P \rangle \langle G \rangle + \langle \kappa_P' G' \rangle$.

In the present study, we explore TRI in a statistically, one-dimensional nonstationary turbulent nonpremixed system using DNS. The principal quantities examined are the normalized means $\mathcal{R}_{T^4}$, $\mathcal{R}_{\kappa I_b}$, and $\mathcal{R}_{\kappa G}$,

$$\mathcal{R}_{T^4} \equiv \frac{\langle T^4 \rangle}{\langle T \rangle^4} \; , \; \mathcal{R}_{\kappa I_b} \equiv \frac{\langle \kappa_P' I_b' \rangle}{\langle \kappa_P \rangle \langle I_b \rangle} \; , \; \mathcal{R}_{\kappa G} \equiv \frac{\langle \kappa_P' G' \rangle}{\langle \kappa_P \rangle \langle G \rangle} \; . \tag{3}$$

In the absence of TRI, $\mathcal{R}_{T^4}$ would be equal to one, and $\mathcal{R}_{\kappa I_b}$, and $\mathcal{R}_{\kappa G}$ would each be equal to zero. The departures of each quantity from these values allow different contributions to TRI to be isolated and quantified.

A dimensionless optical thickness κL is introduced, where L is an appropriate length scale. Kabashnikov and coworkers [13–15] suggested that if the mean free path for radiation is much larger than the turbulence eddy length scale, then the fluctuations in κ (a quantity dependent on local properties) should be uncorrelated with those in G (a nonlocal quantity), so that $\langle \kappa G \rangle \approx \langle \kappa \rangle \langle G \rangle$: this is the "optically thin fluctuation approximation" or OTFA ($\kappa L \ll 1$). At the other extreme ($\kappa L \gg 1$), the optical thickness may be large compared to *all* hydrodynamic and chemical scales. In that case, fluctuations in intensity are generated locally and would be expected to be correlated strongly with those of the absorption coefficient: a diffusion approximation is appropriate in that case [1]. Between these extremes are cases where the smallest scales (Kolmogorov microscales and/or flame thickness) are optically thin while the largest (integral scales) are optically thick. Modeling of such intermediate cases is an outstanding challenge in TRI, and is the primary motivation for this study.

3. Statistically One-Dimensional Nonpremixed Flame

3.1. Computational Configuration

A statistically one-dimensional, nonstationary (decaying), turbulent nonpremixed system is considered (Fig. 1). The configuration is a cube of sides 2π with 64 grid nodes in the y- and z-direction and 65 grid nodes in the x-direction. The boundaries are periodic in the y- and z-directions and nonreflecting in the x-direction [16]. For radiation, the x-direction boundaries are considered cold: radiation incident on those boundaries is absorbed, while no emission occurs at the boundary.

3.2. Physical Models

The continuity, linear momentum, chemical species, and energy equations have the same form as in [17]. Nondimensional forms of the governing equations are solved. An initial turbulence spectrum is prescribed using methods outlined in [17, 18]. The chemistry and the radiation are coupled to the fluid dynamics, i.e., the chemical and radiative source terms feed back into the energy equation. A one-step irreversible reaction is considered, wherein fuel (F) and oxidizer (O) react to form products (P):

$$F + O \rightarrow P. \tag{4}$$

A one-dimensional laminar nonpremixed flame is initialized using analytical expressions from the asymptotic analysis performed by Cuenot and Poinsot [19] for single-step reaction with finite−rate chemistry using a classical Arrhenius model to calculate the reaction rate. All thermodynamic and chemical quantities of a diffusion flame with variable density, unity Lewis number and finite−rate chemistry are obtained from this analysis. The Damköhler number, Da,

for the reaction is 237.88. Standard molecular transport models (Newtonian viscosity, Fourier conduction, and Fickian species diffusion) are employed, where the molecular transport coefficients (viscosity μ, thermal conductivity λ, and species diffusion coefficient $\mathcal{D}$) are set such that the Prandtl number $Pr = 0.75$ and Lewis number $Le = 1.0$ are constant. The viscosity of the fluid depends on the temperature. Soret and Dufour effects are not included. The working fluid is an ideal gas with constant ratio of specific heats, $\gamma = 1.4$.

Radiation properties correspond to a fictitious nonscattering gray gas with Planck-mean absorption coefficient of

$$\kappa_p = C_\kappa (Y_P + \epsilon_Y) \left[c_0 + c_1 \left(\frac{A}{T}\right) + c_2 \left(\frac{A}{T}\right)^2 + c_3 \left(\frac{A}{T}\right)^3 + c_4 \left(\frac{A}{T}\right)^4 + c_5 \left(\frac{A}{T}\right)^5 \right] . \qquad (5)$$

Coefficients A and c_0–c_5 have been taken from a radiation model suggested for water vapor [20]. Here Y_P is the product mass fraction, ϵ_Y is an arbitrary, small, positive threshold to ensure that κ_P is nonzero everywhere, and C_κ is a coefficient that allows the optical thickness to be varied systematically and independently of other parameters. For fixed values of C_κ and Y_P, κ_P varies by more than a factor of ten over the temperature range of interest (the nondimensional $T_{min} = 2.5$ and $T_{max} = 10.0$ correspond to 300 K and 1200 K, respectively). An optical thickness κL based on burned-gas ($Y_P = 1.0$) properties and the initial turbulence integral length scale L characterizes thermal radiation. Simulation parameters are summarized in Table 1. The correlations of Eq. (3) are studied for three values of the optical thickness: (a) an optically thick case, $\kappa L = 10$; (b) optically intermediate case, $\kappa L = 1$; and (c) optically thin case, $\kappa L = 0.1$. The turbulent Reynolds number is defined as $Re = u'_{rms} L/\nu$, where u'_{rms} is the RMS turbulence velocity for the initial turbulent field and ν is kinematic viscosity.

Table 1 *Simulation parameters. In all cases:* $Da = 237.88$, Pr *= 0.75,* Le *= 1.0, and* γ *= 1.4.*

Case	Grid	κL	L	Re_0
Case 1	$65 \times 64 \times 64$	10.0	0.52	105.
Case 2	$65 \times 64 \times 64$	1.0	0.52	105.
Case 3	$65 \times 64 \times 64$	0.1	0.52	105.

3.3. Numerical Methods

Temporal integration is performed with a Runge-Kutta method of order three; for spatial discretization, a compact scheme of order six is used in the interior of the computational domain with noncentered schemes near boundaries [16]. Details of the equations, normalizations, and numerical methods (in the absence of thermal radiation) can be found in [18].

The RTE is solved using a photon Monte Carlo method, wherein the trajectories of a large number of representative photon bundles generated using statistical sampling techniques are

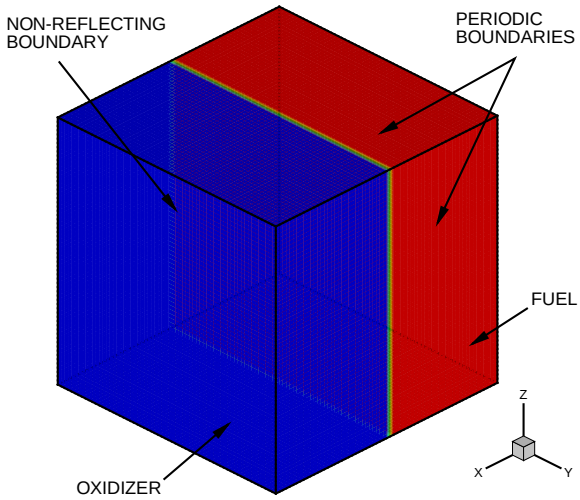

Figure 1 *Configuration for the one-dimensional flame*

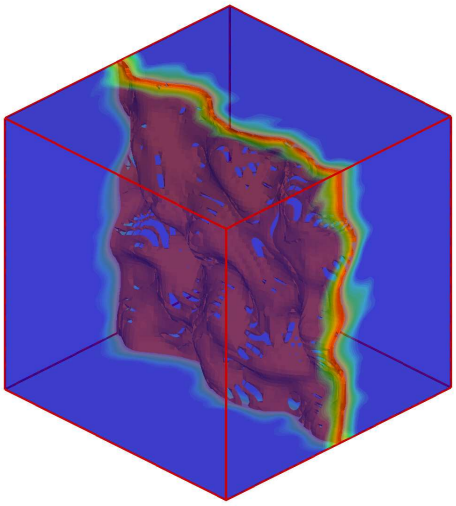

Figure 2 *Product mass fraction, Y_P profile and iso-surface at $Y_P = 0.9$ at time $t/\tau = 1.36$*

followed [1, 11, 12]. The photon Monte Carlo method for a participating medium consists of two parts: an emission stage and a tracing/absorption stage. For the periodic boundaries that are considered here, a photon bundle that exits through one face simply reenters the corresponding location on the opposite face with its direction and properties unchanged. Each emitted photon bundle is traced until its energy is depleted to a near-zero threshold. Details of the photon Monte Carlo method, including issues of numerical accuracy and computational efficiency, can be found in [12]. Here third-order accurate schemes in space have been employed for the photon Monte Carlo method.

4. Results and Discussion

The numerical simulations were carried out using a $65 \times 64 \times 64$ computational grid, and tracing 10^7 photon bundles per time step. A parallel implementation using MPI was used to speed up the photon Monte Carlo calculations. Mean quantities are estimated by averaging over all grid points in the y-z plane for each x-location for this statistically one-dimensional configuration. The simulations proceed from the initial condition as shown in Fig. 1. Fuel and oxidizer react to form products and, due to the imposed turbulence, the flame wrinkles as shown in Fig. 2. Simulations are stopped at $t/\tau = 1.36$ because of the limitations of the boundary conditions in the x-direction. Here t/τ is the nondimensional time normalized by the initial eddy turn over time τ, where $\tau = L/u'_{rms}$. The x-direction boundaries are considered cold for radiation and, hence, care must be taken to run the simulations only as long as this assumption remains valid. If the simulations are run any longer, then the reactants at the boundaries will get preheated and the wrong boundary condition would be used, giving erroneous results.

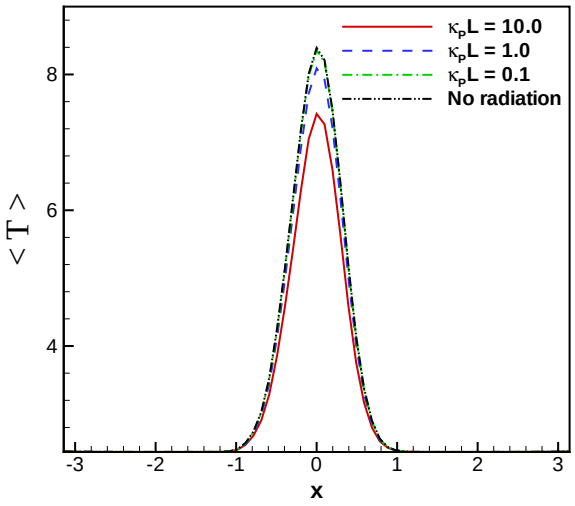

Figure 3 *Mean temperature along the x-direction for three values of optical thickness at $t/\tau = 1.36$ and for the case without radiation*

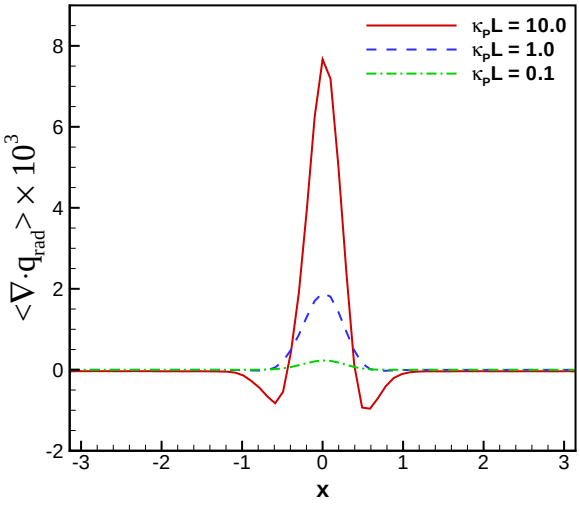

Figure 4 *Mean radiative source term along the x-direction for three values of optical thickness at $t/\tau = 1.36$*

Figure 3 shows the plane-averaged mean temperature at $t/\tau = 1.36$, the end of the simulation, along the x-direction. The peak mean temperature for the optically thick case is the lowest indicating that radiative losses have cooled the hot products more than that at other optical thicknesses. The peak mean temperature for the optically thin case is almost identical to that for the case without radiation feedback, while the peak mean temperature for the optically intermediate case lies in between those for the optically thick and optically thin cases. This is further explained by the trend in the mean radiative source term for the three optical thicknesses along the x-direction as shown in Fig. 4.

4.1. Emission TRI

Emission TRI quantities, discussed in Section 2**,** are determined for the three simulations and compared. Figure 5 shows the temperature self-correlation factor $\mathcal{R}_{T^4}$ at $t/\tau = 1.36$. It is unity in the pure reactants, indicating no TRI in this region as fluctuations in this region are minimal. $\mathcal{R}_{T^4}$ increases rapidly to a peak value of about 2.9 at $x = -0.5$ and of about 2.6 at $x = 0.5$ in the diffusion region near the flame for the optically thin case. The temperature in this region increases rapidly due to the transport of hot products from the flame, the preheating of reactants due to the chemical heat release and the radiative emission. Since the plot is an instantaneous snapshot in time, the two peaks are not equal, indicating the flame wrinkling more on one side than the other. Also, the peak values decreases with increasing optical thickness. This indicates that in addition to decrease in temperature, the fluctuations are smoothened out with increasing optical thickness. The correlation factor decays back to about 1.3 in the flame region at $x = 0.0$. Here there are mostly hot products and hence the fluctuations in the temperature are reduced as

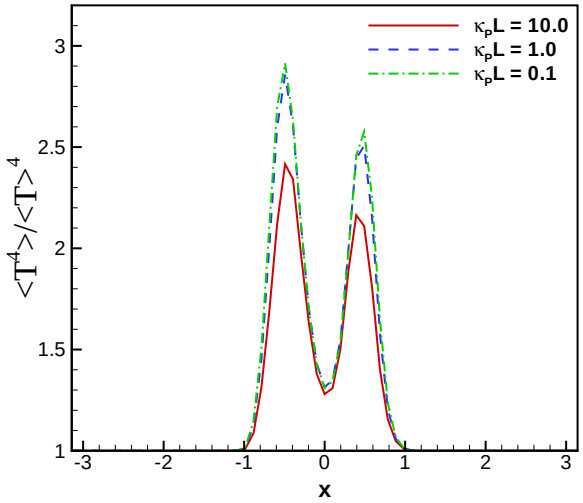

Figure 5 *Temperature self-correlation along the x-direction for three values of optical thickness at $t/\tau = 1.36$*

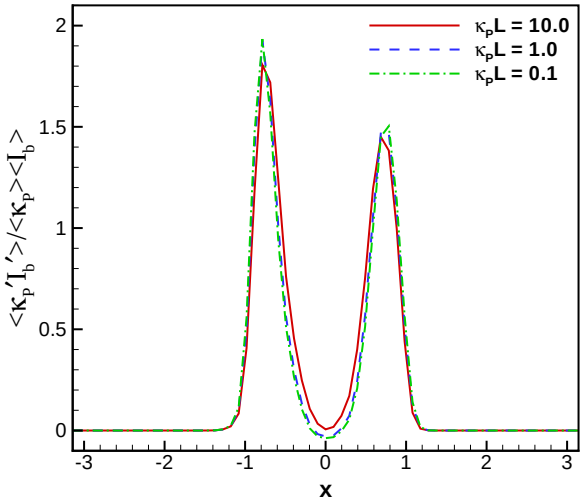

Figure 6 *Absorption coefficient–Planck function correlation factor $\mathcal{R}_{\kappa I_b}$ along the x-direction for three values of optical thickness at $t/\tau = 1.36$*

compared to the diffusion region. The trend is almost the same but not identical for all the three different optical thicknesses. This suggests that the temperature fluctuations are unaffected by optical thickness in this region.

Figure 6 shows the absorption coefficient−Planck function correlation factor $\mathcal{R}_{\kappa I_b}$ at $t/\tau = 1.36$ and shows similar trends to that for temperature self-correlation factor. $\mathcal{R}_{\kappa I_b}$ is very close to zero far from the flame where the reactants are cold and the fluctuations are induced by the turbulence only. The correlation factor rises rapidly in the diffusion region and reaches a peak, which indicates the emission is enhanced due to TRI here. In the region very close to the flame, the correlation factor decreases below zero, indicating that emission is suppressed due to TRI. This can be explained from the functional form of the Planck-mean absorption coefficient $\kappa_P(Y_P, T)$, where there is a competing effect of Y_P and T on κ_P. The absorption coefficient increases with Y_P when the rest of the parameters are held constant, but it decreases with T. For low values of Y_P and T, indicative of reactants, the absorption coefficient is influenced actively by Y_P and hence, the value of the absorption coefficient increases although both Y_P and T are increasing. For high values of Y_P and T, indicative of products, the absorption coefficient is influenced actively by T and, hence, the value of the absorption coefficient decreases even though both Y_P and T are increasing. This results in the negative value of the correlation factor in the flame zone. The trends are almost same for all three optical thicknesses as in the case for the temperature self-correlation factor.

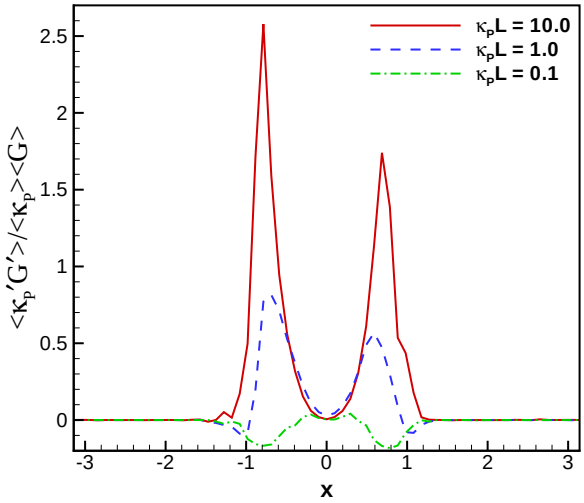

Figure 7 *Absorption coefficient–intensity correlation factor $\mathcal{R}_{\kappa G}$ along the x-direction for three values of optical thickness at $t/\tau = 1.36$*

4.2. Absorption TRI

Absorption TRI effects, shown in Fig. 7, also show trends similar to those of emission TRI, but vary significantly with the change in the optical thickness with the correlation factor decreasing with decreasing optical thickness. This is explained as follows: in the optically thick case, the emitted radiation is mostly locally absorbed or travels a small distance before being absorbed. The fluctuations in the incident radiation G, a nonlocal quantity, are highly correlated with those of the absorption coefficient κ_P, a local quantity. Hence, the TRI effects for absorption are similar to those observed by emission. In the optically thin case, emitted radiation travels to the end of the domain with only a small fraction of it being absorbed. The fluctuations in the incident radiation G are weakly correlated with those of the absorption coefficient κ_P. Thus, absorption TRI effects are very small for the optically thinnest case. The TRI effects for the optically intermediate are in between those observed for the optically thick and the optically thin cases. This trend is different than that seen in emission TRI.

4.3. Net TRI

In studies using modeling approaches such as RANS, only the mean properties are known. In such scenarios, corresponding to no TRI, the radiation calculations are performed based on the mean properties, i.e., $\kappa_P(\langle Y_P \rangle, \langle T \rangle)$ and $I_b(\langle T \rangle)$, and the corresponding radiative source term is $\langle \nabla \cdot \vec{q}_{rad} \rangle_{NO\ TRI}$. The net difference between TRI and no TRI is plotted in Fig. 8 for the three optical thicknesses (considering only $-1.0 < x < 1.0$, the diffusion region around the flame), and the difference is normalized by the emission term without TRI, $\langle \kappa_P I_b \rangle_{NO\ TRI} = \langle \kappa_P(\langle Y_P \rangle, \langle T \rangle) I_b(\langle T \rangle) \rangle$. The net TRI effect is strongest for the optically intermediate case,

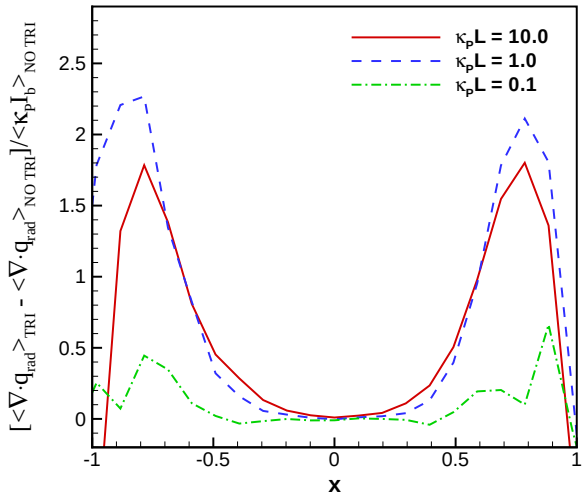

Figure 8 *Net TRI along the x-direction for three values of optical thickness at $t/\tau = 1.36$*

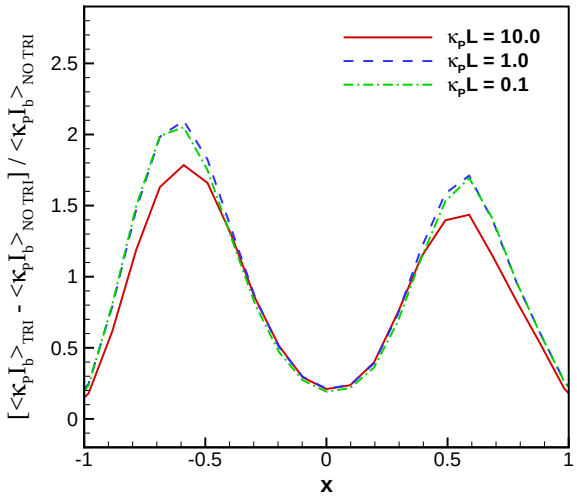

Figure 9 *Emission TRI along the x-direction for three values of optical thickness at $t/\tau = 1.36$*

significant for optically thick, and the least for optically thin case, but not zero, for this configuration of a statistically one-dimensional nonpremixed flame. Figure 8 also indicates that the net TRI effect is maximum at the end of the diffusion zone facing the cold reactants and minimum in the hot flame zone for all the three optical thicknesses. The difference between emission with TRI and without TRI, normalized by the emission term without TRI, is shown in Fig. 9. The trends are similar to those seen in Fig. 6. The difference of the two quantities plotted in Figs. 8 and 9 is the difference between absorption with TRI and without TRI normalized by the emission without TRI.

For an idealized problem such as this one, the dynamic range of scales is small. Hence, one must exercise caution in extrapolating DNS results to practical combustion systems. DNS can, however, help in studying the influence of key dimensionless parameters (e.g., Re, Da, κL) and of the functional form of $\kappa_P(Y_P, T)$ and will ultimately help to assess and calibrate models suitable for engineering application.

5. Conclusion

Direct numerical simulation coupled with a radiation photon Monte Carlo method has been used to explore turbulence−radiation interaction in an idealized nonpremixed system. The temperature self-correlation, absorption coefficient−Planck function correlation, and absorption coefficient−intensity correlation have been isolated and quantified to study TRI effects. At intermediate-to-large values of optical thickness, contributions from all three correlations are significant. In the optically thin limit only the temperature self-correlation and absorption coefficient−Planck function correlation are significant. In future work, DNS will be used to explore advanced scenarios involving complex chemistry, nongray-gas radiation and soot radiation.

Acknowledgment

The authors gratefully acknowledge the financial support of the National Science Foundation under Grant Number CTS-0121573.

REFERENCES

[1] MODEST, M. F., *Radiative Heat Transfer*, Academic Press, New York, 2nd edn., 2003.

[2] TOWNSEND, A. A., The Effects of Radiative Transfer on Turbulent Flow of a Stratified Fluid, 4, 361–375, 1958.

[3] SONG, T. H. and VISKANTA, R., Interaction of Radiation with Turbulence: Application to a Combustion System, 1(1), 56–62, 1987.

[4] SOUFIANI, A., MIGNON, P., and TAINE, J., Radiation–Turbulence Interaction in Channel Flows of Infrared Active Gases, in *Proceedings of the Ninth International Heat Transfer Conference*, 6, Washington, D.C., Hemisphere, 403–408, 1990.

[5] HALL, R. J. and VRANOS, A., Efficient Calculations of Gas Radiation From Turnbulent Flames, 37, 2745, 1994.

[6] TIEZSEN, S. R., On the Fluid Mechanics of Fires, *Ann. Rev. Fluid Mech.*, 33, 67–92, 2001.

[7] MAZUMDER, S. and MODEST, M. F., A PDF Approach to Modeling Turbulence–Radiation Interactions in Nonluminous Flames, 42, 971–991, 1999.

[8] LI, G. and MODEST, M. F., Application of composition PDF methods in the investigation of turbulence–radiation interactions, 73, 461–472, 2002.

[9] COELHO, P. J., Detailed numerical simulation of radiative transfer in a nonluminous turbulent jet diffusion flame, 136, 481–492, 2004.

[10] TESSÉ, L., DUPOIRIEUX, F., and TAINE, J., Monte Carlo modeling of radiative transfer in a turbulent sooty flame, 47, 555–572, 2004.

[11] WU, Y., HAWORTH, D. C., MODEST, M. F., and CUENOT, B., Direct Numerical Simulation of Turbulence/Radiation Interaction in Premixed Combustion Systems, *Proceedings of the Combustion Institute*, 30, 639–646, 2005.

[12] WU, Y., MODEST, M. F., and HAWORTH, D. C., A High-Order Photon Monte Carlo Method for Radiative Transfer in Direct Numerical Simulation of Chemically Reacting Turbulent Flows, 2005, submitted.

[13] KABASHNIKOV, V. P. and KMIT, G. I., Influence of Turbulent Fluctuations of Thermal Radiation, 31, 963–967, 1979.

[14] KABASHNIKOV, V. P., Thermal Radiation of Turbulent Flows in the Case of Large Fluctuations of the Absorption Coefficient and the Planck Function, 49(1), 778–784, 1985.

[15] KABASHNIKOV, V. P. and MYASNIKOVA, G. I., Thermal Radiation in Turbulent Flows—Temperature and Concentration Fluctuations, *Heat Transfer-Soviet Research*, 17(6), 116–125, 1985.

[16] LELE, S. K., Compact finite difference schemes with spectral-like resolution, 103, 16–42, 1992.

[17] HAWORTH, D. C. and POINSOT, T. J., Numerical Simulations of Lewis Number Effects in Turbulent Premixed Flames, 104, 111–137, 1996.

[18] BAUM, M., *Etude de l'allumage et de la structure des flammes turbulentes*, PhD thesis, Ecole Centrale, Paris, 1994.

[19] CUENOT, B. and POINSOT, T., Asymptotic and Numerical Study of Diffusion Flames with Variable Lewis Number and Finite Rate Chemistry, 104, 111–137, 1996.

[20] COMBUSTION RESEARCH FACILITY, S. N. L., *Intern'l. Workshop on Measurement and Computation of Turbulent Nonpremixed Flames*, 2002.